ATLAS NOTE

July 11, 2010

ATLAS sensitivity prospects to W' and Z' in the decay channels $W' \to \ell\nu$ and $Z' \to \ell^+\ell^-$ at $\sqrt{s} = 7$ TeV

The ATLAS collaboration

ATL-PHYS-PUB-2010-007
11 July 2010

Abstract

The ATLAS sensitivities to a high-mass dilepton resonance, and to a lepton-neutrino resonance, are evaluated using full detector simulation. These evaluations use, as benchmarks, models in which new heavy gauge bosons (denoted as W' and Z') have the same couplings as their Standard Model counterparts. In both cases (W', Z'), at the center-of-mass energy of the initial LHC run (7 TeV), ATLAS is found to be sensitive to a mass range significantly higher than the current limits from direct searches. A total integrated luminosity of 50 pb^{-1} is found to be enough to extend the W' exclusion to 1.5 TeV; 100 pb^{-1} would be enough to extend the Z' exclusion to 1.3 TeV.

1 Introduction

Although the Standard Model (SM) of the strong and electroweak interactions describes particle physics at energies attainable so far, the model is not a complete theory. For example, it does not explain the number of lepton and quark generations nor their mass hierarchy, and many constants in the model are unconstrained. It is therefore important for the ATLAS physics program to look for indications of physics beyond this theoretical framework. Some of the theories proposed to address the above shortcomings contain gauge symmetries that can be spontaneously broken, and that correspond to additional gauge bosons; in particular, any charged, spin 1 gauge boson which is not included in the SM is called a W', and a neutral, spin 1, non-SM gauge boson is customarily denoted as Z'.

This document summarizes the ATLAS physics potential for the search of these bosons through their leptonic decays; *i.e.*, for the search of high-mass dilepton or lepton-neutrino resonances. In what follows, unless otherwise mentioned, *lepton* is used to denote an electron or a muon of either charge.

To evaluate the sensitivities, this study uses 'SM-like' models; *i.e.*, models in which the new gauge bosons have the same fermion couplings as their SM counterparts [1], quoted as Sequential Standard Models (SSM). Therefore, in both cases considered, the diboson decays are suppressed.

The DØ experiment at Fermilab has published the present direct search lower limit for the W' boson mass [2] as $m_{W'} > 1$ TeV at 95% C.L.. CDF has published the current limit on the mass of a Z' boson as $m_{Z'} > 1$ TeV [3]. Previous ATLAS studies [4, 5] have evaluated the physics potential of these searches at $\sqrt{s}$=14 TeV. This study evaluates the potential at $\sqrt{s}$=7 TeV, which is the center-of-mass energy for the 2010/11 LHC operation, and shows that even in this scenario, a large mass range is accessible beyond the Tevatron limit in the early stages of the LHC run.

The document is organized as follows: Section 2 describes the samples used. Sections 3 and 4 describe briefly the performance for the reconstruction of leptons and missing transverse energy, respectively, and Section 5 the systematic uncertainties. Finally, Sections 6 and 7 present the results of the dilepton and lepton+neutrino searches.

2 Monte Carlo Samples

Simulation and reconstruction of the Monte Carlo data were done with a recent release of the ATLAS software framework, which is very close to what is used for data. The alignment and calibration of the detector are assumed to be well described. Nevertheless, systematic uncertainties are introduced to account for the present knowledge of the detector performance (Section 5), which will be extensively tested and improved as data are recorded.

Table 1 summarizes the samples used in this study. All cross sections used for this study are LO, except the $t\bar{t}$ one, which is NLO. The generator level information of these samples was produced with a center of mass energy of 10 TeV. To evaluate the 7 TeV sensitivities using the Monte Carlo samples available, which were generated at a center-of-mass energy of 10 TeV, an event-by-event PDF reweighting procedure was used.

In general, the predicted cross-sections reported by a Monte Carlo generator are computed according to

$$\sigma_{\text{Hadronic}} = \int f_1(x_1, Q) f_2(x_2, Q) \sigma_{\text{Partonic}}(x_1, x_2, Q, \Pi)\, dx_1 dx_2 d\Pi \tag{1}$$

where x_1 and x_2 are the momentum fractions carried by the partons, Q is the QCD scale of the event, and Π denotes the available phase space for the final state. The integral is evaluated by randomly sampling the phase space of the initial and final state, computing the integrand for each point, and taking a suitably weighted sum over the results.

Process	Generator	$\sigma \times BR$ [fb]	Comments	Events
$Z' \to e^+e^-$ [1.0TeV]	PYTHIA [6]	248.6	$min(\sqrt{s'}) = 500\,\text{GeV}$	30k
$Z' \to e^+e^-$ [1.5TeV]	PYTHIA	76.1	$min(\sqrt{s'}) = 500\,\text{GeV}$	15k
$Z' \to \mu^+\mu^-$ [1.0TeV]	PYTHIA	251.5	$min(\sqrt{s'}) = 500\,\text{GeV}$	30k
$Z' \to \mu^+\mu^-$ [1.5TeV]	PYTHIA	77.8	$min(\sqrt{s'}) = 500\,\text{GeV}$	15k
Drell Yan e^+e^-	PYTHIA	81.78	$400 < m_{ll} < 600\,\text{GeV}$	10k
Drell Yan e^+e^-	PYTHIA	16.28	$600 < m_{ll} < 800\,\text{GeV}$	10k
Drell Yan e^+e^-	PYTHIA	4.487	$800 < m_{ll} < 1000\,\text{GeV}$	10k
Drell Yan e^+e^-	PYTHIA	1.762	$1000 < m_{ll} < 1250\,\text{GeV}$	10k
Drell Yan e^+e^-	PYTHIA	0.5496	$1250 < m_{ll} < 1500\,\text{GeV}$	10k
Drell Yan e^+e^-	PYTHIA	0.1982	$1500 < m_{ll} < 1750\,\text{GeV}$	10k
Drell Yan e^+e^-	PYTHIA	0.0764	$1750 < m_{ll} < 2000\,\text{GeV}$	10k
Drell Yan e^+e^-	PYTHIA	0.0570	$m_{ll} > 2000\,\text{GeV}$	10k
Drell Yan $\mu^+\mu^-$	PYTHIA	88.01	$400 < m_{ll} < 600\,\text{GeV}$	20k
Drell Yan $\mu^+\mu^-$	PYTHIA	16.74	$600 < m_{ll} < 800\,\text{GeV}$	20k
Drell Yan $\mu^+\mu^-$	PYTHIA	4.611	$800 < m_{ll} < 1000\,\text{GeV}$	20k
Drell Yan $\mu^+\mu^-$	PYTHIA	1.780	$1000 < m_{ll} < 1250\,\text{GeV}$	19k
Drell Yan $\mu^+\mu^-$	PYTHIA	0.5618	$1250 < m_{ll} < 1500\,\text{GeV}$	20k
Drell Yan $\mu^+\mu^-$	PYTHIA	0.1994	$1500 < m_{ll} < 1750\,\text{GeV}$	18k
Drell Yan $\mu^+\mu^-$	PYTHIA	0.0776	$1750 < m_{ll} < 2000\,\text{GeV}$	16k
Drell Yan $\mu^+\mu^-$	PYTHIA	0.0563	$m_{ll} > 2000\,\text{GeV}$	20k
$W' \to \ell\nu$ [1.0TeV]	PYTHIA	4678	—	50k
$W' \to \ell\nu$ [1.5TeV]	PYTHIA	720	—	35k
$W' \to \ell\nu$ [2.0TeV]	PYTHIA	155	—	50k
$W' \to \ell\nu$ [2.5TeV]	PYTHIA	39.8	—	20k
$W' \to \ell\nu$ [3.0TeV]	PYTHIA	11.7	—	20k
SM $W \to \ell\nu$	PYTHIA	12600	$200\,\text{GeV} < m(W) < 500\,\text{GeV}$	50k
SM $W \to \ell\nu$	PYTHIA	390	$m(W) > 500\,\text{GeV}$	50k
Dijet J0	PYTHIA	1.17×10^{13}	$\hat{p_T} = 8 - 17\,\text{GeV}$	999k
Dijet J1	PYTHIA	8.64×10^{11}	$\hat{p_T} = 17 - 35\,\text{GeV}$	998k
Dijet J2	PYTHIA	5.6×10^{10}	$\hat{p_T} = 35 - 70\,\text{GeV}$	959k
Dijet J3	PYTHIA	3.29×10^{9}	$\hat{p_T} = 70 - 140\,\text{GeV}$	1357k
Dijet J4	PYTHIA	1.52×10^{8}	$\hat{p_T} = 140 - 280\,\text{GeV}$	459k
Dijet J5	PYTHIA	5.08×10^{6}	$\hat{p_T} = 280 - 560\,\text{GeV}$	1380k
Dijet J6	PYTHIA	1.12×10^{5}	$\hat{p_T} = 560 - 1120\,\text{GeV}$	399k
Dijet J7	PYTHIA	1.07×10^{3}	$\hat{p_T} = 1120 - 2240\,\text{GeV}$	398k
Dijet J8	PYTHIA	1.1	$\hat{p_T} > 2240\,\text{GeV}$	398k
$t\bar{t}$	MC@NLO [7]	202860	One-lepton filter	1980k

Table 1: Monte Carlo samples used for the study of heavy W' and Z' bosons. The cross sections correspond to a 10 TeV center-of-mass energy. The "One-lepton filter" for the $t\bar{t}$ sample is a generator-level filter that requires each event to contain at least one charged lepton (from a W decay, which should come from top) with p_T above 1 GeV.

The reweighting procedure is based on the observation that the integrand for the cross-section at a different center-of-mass energy is essentially the same, but with x_1, x_2, f_1, and f_2 replaced by values

appropriate for the new center-of-mass energy. In particular, one can write

$$\sigma'_{\text{Hadronic}} = \int R f_1(x_1,Q) f_2(x_2,Q) \sigma_{\text{Partonic}}(x_1,x_2,Q,\Pi)\, dx_1 dx_2 d\Pi \tag{2}$$

where

$$R = \frac{f'_1(x'_1,Q)\, f'_2(x'_2,Q)}{f_1(x_1,Q)\, f_2(x_2,Q)} \tag{3}$$

where x'_1 and x'_2 are the momentum fractions (at the new center-of-mass energy) carried by partons with the same momenta as partons which carry momentum fractions x_1 and x_2 at the old center-of-mass energy. Thus, the cross-section at the new center-of-mass energy is just a differently weighted sum based on the same fully-simulated events.

This procedure was cross checked by rescaling fast simulated Monte Carlo samples produced at the two center-of-mass energies and consistent results were found.

2.1 Z' signals, backgrounds

Z' boson samples where Z' decays into $\ell^+\ell^-$ ($\ell = e, \mu$) were generated for $m_{Z'}$ of 1.0 and 1.5 TeV, using PYTHIA v6.403 [6], with the parton distribution functions CTEQ6L [8]. The main background for the search of a dilepton resonance is the high invariant mass tail of the Drell-Yan process; eight samples, each one covering different intervals of dilepton invariant mass, were used to account for it; Table 1 indicates the mass bins used.

2.2 W' signals, backgrounds

Signal samples of $W' \to \ell\nu$ (where ℓ represents any type of lepton, τ included), were generated with PYTHIA v6.403, using the parton distribution functions CTEQ6L. W' masses ranging from 1.0 to 2.0 TeV were considered.

The main background for this search is the high mass, off-shell tail of the Standard Model W boson. Since this is a steeply falling distribution, and it is important to provide enough background for a large range of masses, two samples were produced each covering a different region of the true invariant mass of the W boson (m_W): 200 GeV $< m_W <$ 500 GeV, and $m_W >$500 GeV.

QCD dijet production could also mimic this signature if a jet fakes an isolated lepton, or if it provides a true isolated lepton that is then misreconstructed as having a much larger momentum (and hence providing a large amount of missing transverse energy).

Boosted or high mass off shell Z decays, where one lepton escapes reconstruction, contribute also to the background for this process. This background behaves as the irreducible one and has been estimated to be $\leq 5\%$ and $\leq 10\%$ of the W tail for the e^+e^- and $\mu^+\mu^-$ channels, respectively.

2.3 Common backgrounds

One potentially important background to both searches is $t\bar{t}$ production, which can produce two leptons, as well as a lepton and missing energy. To account for this process, a sample with a generator-level filter requiring one lepton was used.

The potential background due to cosmic rays is not included in this study. Criteria have been developed with the first recorded data, that allow the heavy suppression of this contribution to the background.

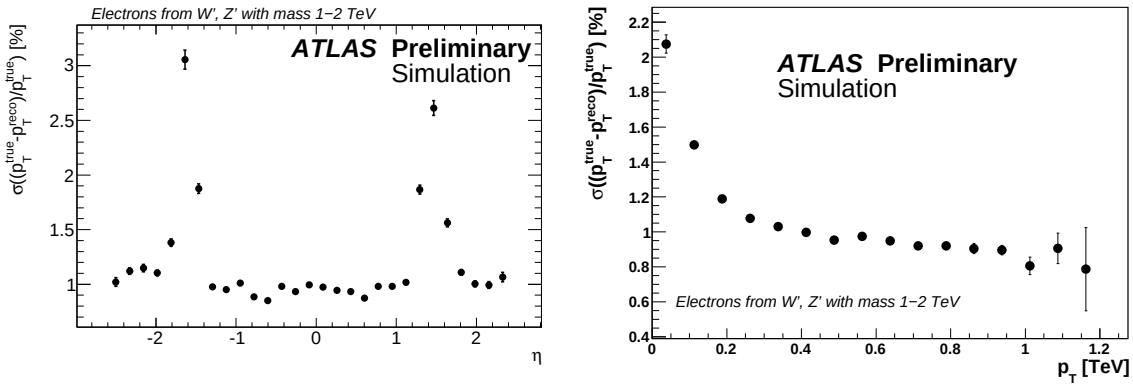

Figure 1: p_T resolution as a function of true η and p_T for high-p_T electrons from W' and Z' decays.

3 Lepton reconstruction at high p_T

3.1 Electron reconstruction

Electron identification and reconstruction procedures in ATLAS are described in detail in [5], where three sets of cuts designed for physics searches are presented. The present study uses the "medium" set of cuts, which include the size of the cluster of calorimeter cells, containment, association with an Inner Detector track, shower shape cuts and quality of the track-cluster match.

For energies in the range considered, the energy resolution of reconstructed electrons is roughly proportional to the square root of the energy deposited; as a result, the width of the *fractional* energy deviation decreases as a function of the true electron energy (it behaves as $1/\sqrt{E}$, with a limiting constant term of $O(1\%)$ that depends on the uniformity of the calorimeter's response). Figure 1 shows, for electrons coming from the W' and Z' signal samples under consideration, the p_T resolution as a function of the electron's true pseudorapidity, η, and true transverse momentum, p_T. Each point in these plots shows the width of a single-Gaussian fit to the core of the distribution of the quantity $(p_T^{\text{reco}} - p_T^{\text{true}})/p_T^{\text{true}}$ (*fractional deviation*, in what follows) in the bin indicated on the horizontal axis.

As expected, the fractional momentum deviation for electrons becomes narrow as the transverse momentum increases. The average resolution for electrons in the momentum range of interest for the W' and Z' searches is expected to be close to 1%. As illustrated in Fig. 1, it is significantly worse in the transition region between the two calorimeter systems (at $|\eta| \sim 1.5$).

Figures 2 and 3 show the efficiency of electron identification and reconstruction as a function of true pseudorapidity (η), azimuthal angle (ϕ) and transverse momentum (p_T) for electrons from W' and Z' boson decays (for the "medium" set of cuts, with no cut on p_T and a requiring $|\eta| < 2.47$). These results were obtained from Monte Carlo samples generated with a center-of-mass energy of 10 TeV, but they depend only weakly on the center of mass energy because they are obtained as a function of lepton p_T and η.

3.2 Muon reconstruction

As described in [5], muon reconstruction in ATLAS uses all main detector subsystems, yielding high efficiency and good momentum resolution for muons with p_T up to $O(1$ TeV). The reconstruction of high p_T muons is seeded by hits in the Muon Spectrometer (MS) and refined using information from the Inner Detector (ID) which improves the momentum resolution and reduces the fake muon rate. Since the reconstruction uses information from two detectors (MS and ID), these muon candidates are called *combined* muons. All the plots of this section, concern combined muons with $|\eta| < 2.5$ and no explicit

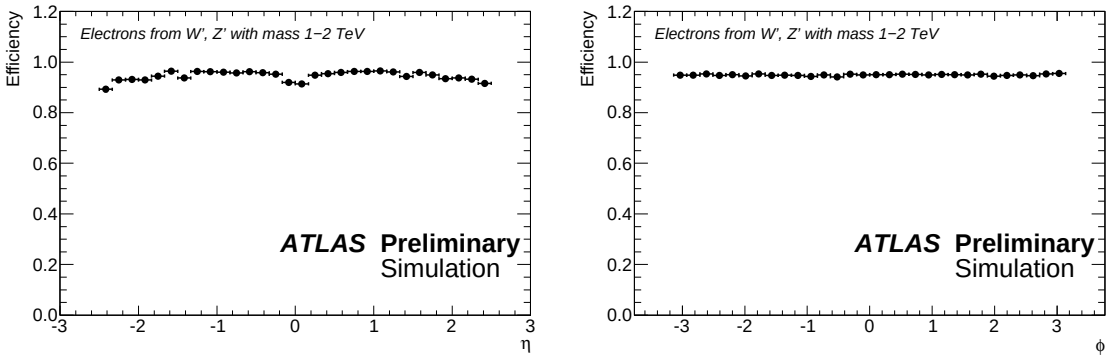

Figure 2: Reconstruction efficiency as a function of η and ϕ for electrons from W' and Z' boson decays.

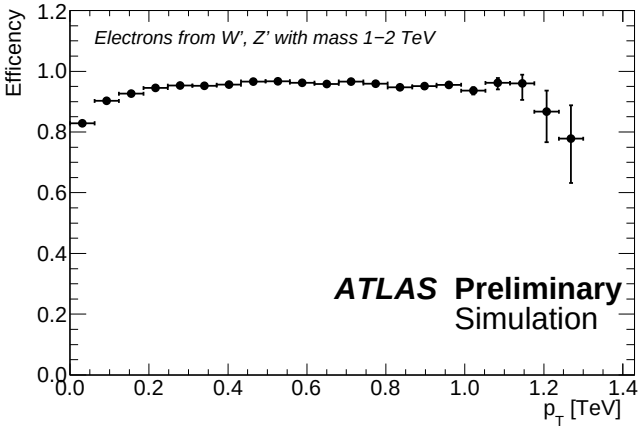

Figure 3: Reconstruction efficiency as a function of p_T for electrons from W' and Z' boson decays.

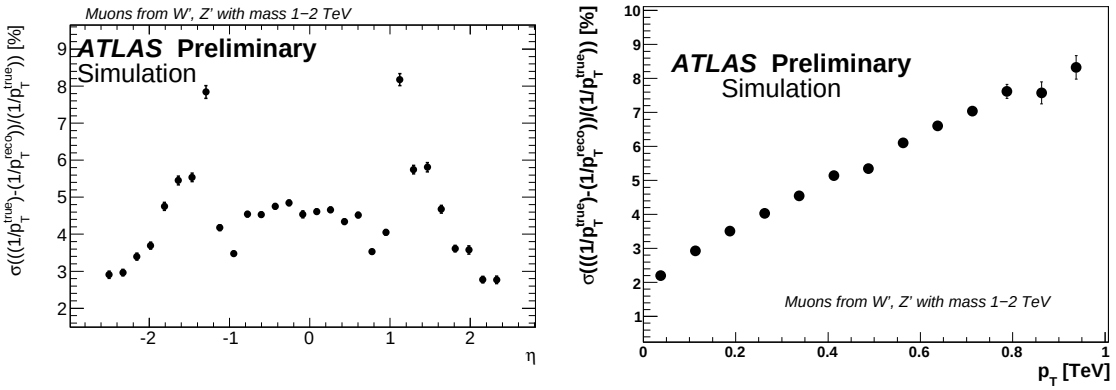

Figure 4: p_T^{-1} resolution for muons from W' and Z' decays as a function of their true η and p_T.

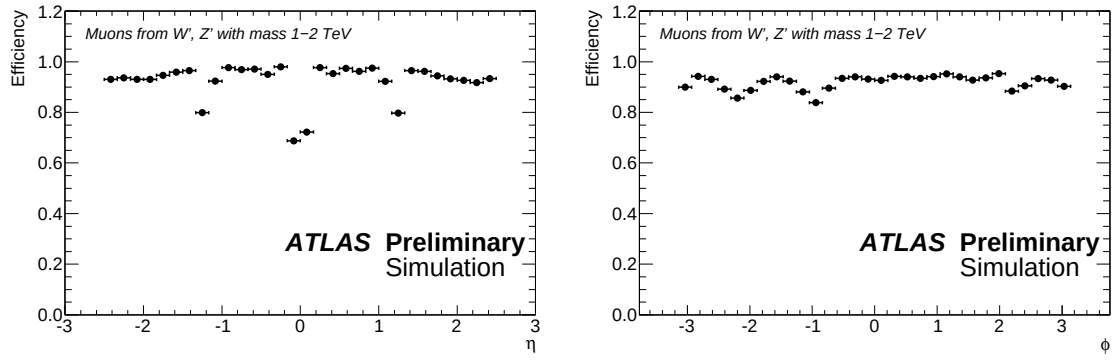

Figure 5: Reconstruction efficiency as a function of η and ϕ for muons from W' and Z' boson decays.

cut on p_T.

The momentum of a muon is measured through the curvature of the corresponding track, which is built from MS and ID hits. The curvature is proportional to $1/p_T$, and therefore this variable is used to present the quality of muon reconstruction. Figure 4 shows the resolution of the fractional deviation of p_T^{-1} for muons coming from W' and Z' bosons. The resolution is degraded at intermediate pseudorapidity ($1.2 < |\eta| < 1.7$) because of the low field integral in the overlap region between barrel and endcap toroids. In contrast to the case of electrons, the width of this fractional deviation becomes larger as the p_T of the muons grows. Consequently, one can expect the reconstruction of high-mass dimuon resonance to be wider than its dielectron counterpart.

Figures 5 and 6 show the efficiency for combined muon reconstruction as a function of pseudorapidity (η), azimuthal angle (ϕ) and transverse momentum (p_T) for muons from W' and Z' boson decays. As in the case of electrons, these results were obtained from Monte Carlo samples generated with a center-of-mass energy of 10 TeV, but depend only weakly on the center of mass energy because they are obtained as a function of lepton p_T and η. Lower efficiencies are observed, as expected, around $|\eta| = 0$ due to the passage of services, and in the transition region between the MS barrel and endcap ($|\eta| \sim 1.2$). The support structures of the detector cause a reduction of the efficiency at the ϕ values where they are located. The decreasing efficiency observed in Fig. 6 as a function of p_T is due to the increase of bremsstrahlung radiation at higher momentum. Large showering inside the MS can either create problems in the pattern recognition, or lead to mis-measured track parameters and a consequent failure in the matching of the ID and the MS tracks.

A poorly reconstructed muon, whose momentum is strongly overestimated, will provide both a high p_T object and large missing transverse energy $\not{E}_T$, which could end up as a spurious W' boson candidate.

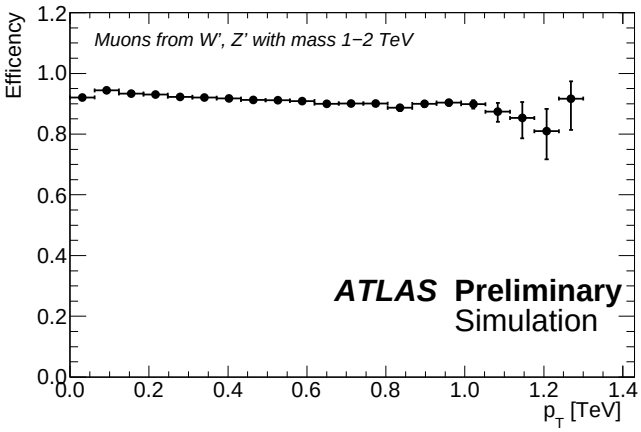

Figure 6: Reconstruction efficiency as a function of p_T for muons from W' and Z' boson decays.

To reduce the probability of this effect, quality criteria were imposed on the following muon quantities:

- The matching χ^2 between MS and ID tracks.
- The impact parameter in the *z*-axis (*i.e.*, the beam axis).

4 Missing Transverse Energy for high p_T electron and muon events

For the W' analysis, the final state under consideration includes a neutrino, whose momentum information can be inferred only from the energy imbalance in the detector.

The total missing energy, $\not{E}_T$, is calculated from energy deposits in calorimeter cells that survive a noise suppression procedure, with corrections applied for muon energy loss and for the energy deposition in the cryostat material; in a second step a refined calibration of the energy in the calorimeter cells is applied, based on their association with reconstructed objects.

A "muon term" is calculated from the momentum of the combined muons (except when the muon is near some hadronic activity, in which case the momentum of the corresponding muon spectrometer track is used). For the W' analysis, $\not{E}_T$ resolution depends mainly on the p_T resolution of the reconstructed lepton. In this study, it is assumed that the rest of the ingredients composing the refined calculation of $\not{E}_T$ will be validated by the time ATLAS accumulates the integrated luminosities required for the discovery or exclusion of the W' boson.

5 Systematic uncertainties

Detector related issues for these final states depend mainly on lepton reconstruction uncertainties. Nevertheless, jet reconstruction has also been taken into account both for the W' event selection and the $\not{E}_T$ evaluation. In this study, the same sources of systematic uncertainty listed in [5] are considered, but with modified values to account for the lower statistics available for their evaluation. The values used in [5] were obtained assuming more than 100 pb^{-1} of data; for this study, an integrated luminosity of the order of 10 pb^{-1} is assumed, as this could be the amount of data needed for the exclusion limits or the discoveries of W' or Z' bosons with masses $\sim$1 TeV. Uncertainties of 5% and 10% were used for the identification efficiency of electrons and muons, respectively. Both will be evaluated via the extrapolation of the results obtained by the tag and probe method on real data, but the uncertainty on muons is expected to be higher because the corresponding efficiency is expected to drop as the muon p_T increases due to

the higher radiation probability (see Section 3.2). A 3% energy scale uncertainty is used for both lepton categories. Concerning p_T resolutions, a 100% relative uncertainty was used for electrons. The same uncertainty was used for muons in the end-cap region, where the absolute alignment is already known to a very good level [9]. In what concerns the barrel muons, the whole difference observed in [9] between the expected resolution and the one obtained with the present alignment was used as a systematic uncertainty. The relative uncertainty obtained in this way, reaches the value of 200% for 1 TeV muons and has a visible but moderate effect with respect to the efficiency uncertainty, which is 3% on the signal and 2% on the background for a W' boson mass of 1 TeV. For a W' boson with a mass of 1.5 TeV, the effect is increased to 8% and 7%, respectively. The effect on the dimuon search is smaller, since there is no direct correlation between the two measured muon momenta, as it is the case for the muon+$\not\!\!E_T$ channel, where the muon p_T is highly correlated with the $\not\!\!E_T$ estimation. It should be noted however, that the alignment of the barrel muon spectrometer is expected to improve with the integrated luminosity relevant for this study. A 10% uncertainty was used for the jet energy scale and resolution, which has a negligible effect on the results of this study ($\sim 1\%$). Finally, a 10% uncertainty was assumed for the luminosity.

In summary, the experimental uncertainties with $\sim$10 pb^{-1} of data are expected to be dominated by the lepton identification efficiency and the luminosity uncertainties, which vary in a correlated way for the signal and the backgrounds. For the dilepton study, an overall experimental uncertainty of 14% (21%) is assigned to the electron (muon) channel concerning both the signal and the background. The corresponding values for the lepton+$\not\!\!E_T$ analysis were found to be 11% (15%).

Despite the fact that no K factors are used in this study, the theoretical uncertainties are estimated in the framework of MCFM [10]. The theoretical contribution to the systematic uncertainty was calculated from the Parton Distribution Functions (PDF) uncertainties; the effect of varying the factorization and renormalization scales was calculated as well and found to be negligible in comparison. The PDF uncertainties were obtained from a full NLO calculation for Drell-Yan to dimuons in bins of invariant mass. The uncertainties were obtained using the standalone NLO Monte Carlo calculator MCFM, with the LHAPDF [11] set CTEQ6m [8] NLO PDFs. The NLO symmetric theoretical uncertainty varies from 7%-15% over the search range, with good agreement with the asymmetric uncertainty, as shown in Fig. 7. Previous studies, done for a center-of-mass energy of 14 TeV [5], found that the theoretical uncertainties for the W and W' production are very similar to those from Drell-Yan and Z' production; assuming that this behaviour does not depend on the center of mass energy, this study uses the same mass-dependent theoretical uncertainties (shown above) for both cases.

6 Dilepton search potential

6.1 Event selection

The decay $Z' \to \ell^+\ell^-$ provides a simple and clean signature of two oppositely charged, same flavour high p_T leptons. The invariant mass of the two leptons can be used very effectively to discover the resonance over a rapidly falling background at high masses. The main irreducible background is the high-mass tail of the Drell-Yan process. Other reducible sources of background, that can can lead to two reconstructed leptons in the final state, are $t\bar{t}$ and QCD dijet production (mainly $b\bar{b}$ contributes to the second category). Diboson production can also contribute to the background, but was found to be negligible [5]. The dilepton QCD background contributes heavily at low masses and obscures the control region that will be used to evaluate the Drell-Yan background from the data; on the other hand, due to its very large cross section, it can also become significant in the high mass region if not heavily suppressed. Therefore, a soft isolation cut has been imposed to suppress this background; the cut is also useful to reduce the $t\bar{t}$ background. A simple track isolation procedure, using the sum of the p_T of tracks in a cone of $\Delta R = \sqrt{\Delta\eta^2 + \Delta\phi^2} = 0.3$ around the lepton, divided by the lepton p_T (normalized track

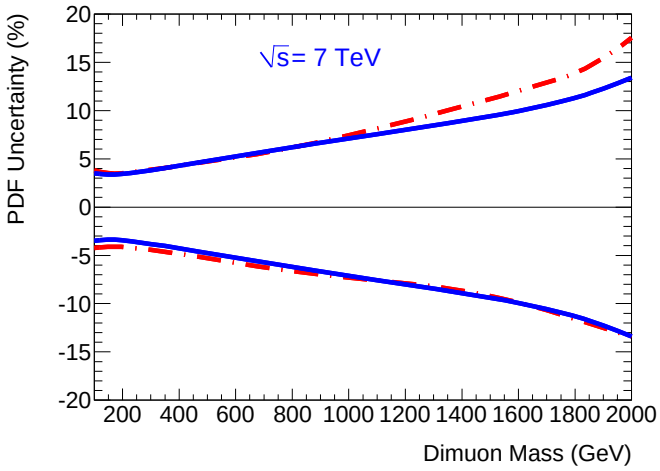

Figure 7: CTEQ6m PDF uncertainties as a function of the dimuon invariant mass for symmetric (solid line) and asymmetric (dash-dot line) uncertainties as calculated by MCFM at center-of-mass energy 7 TeV.

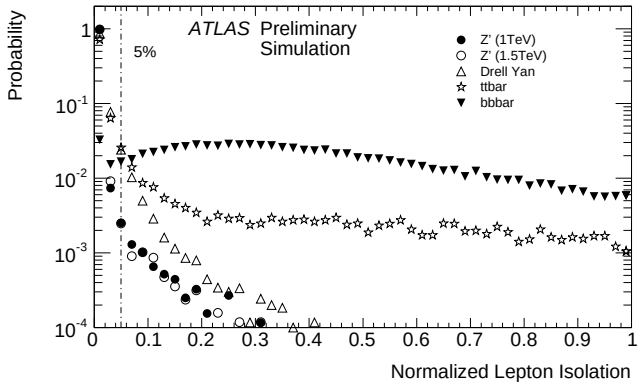

Figure 8: Normalized track isolation distribution for signal and various backgrounds

isolation), was used for this purpose. The distribution of this isolation quantity for the signal and the various backgrounds is shown in Fig. 8. The selection requirements can be summarized as follows:

- Two leptons passing the selection criteria described in Sections 3.1 and 3.2.
- For each lepton, $p_T > 20$ GeV and $|\eta| < 2.5$.
- For each lepton, $\sum_{\Delta R<0.3} p_T^{tracks}/p_T^{lepton} < 0.05$

No explicit charge requirement is imposed because the definition of the charge may suffer from large uncertainty for electrons at the beginning of the LHC operation. Also, the probability of wrongly assigning the charge grows as the p_T of the particles becomes large.

Single lepton triggers can be used to trigger very efficiently on this final state. For example, for the early data taking period, triggers requiring a single lepton over 10 GeV provide an efficiency of $\sim 99\%$ (98%) for the electron (muon) channel for the events that pass the final analysis requirements. Moving the threshold to 20 GeV reduces the efficiency by $\sim$1%. The dilepton invariant mass after the selection specified above is presented in Fig. 9 for the two channels (e^+e^-, $\mu^+\mu^-$) for two values of the true $m(Z')$ (1.0 and 1.5 TeV).

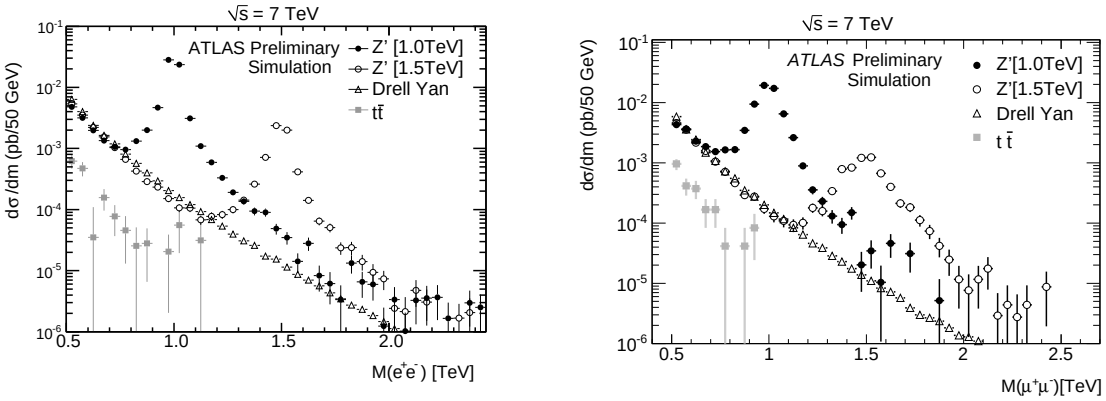

Figure 9: Dilepton invariant mass spectra after all cuts for the electron (left) and muon (right) channels.

6.2 Luminosity for discovery

The potential of the search can be evaluated as a function of the true mass of the Z' boson, by the luminosity needed to observe a signal with a statistical significance of 5σ. The significance is obtained from the expected number of signal and background events for a dilepton invariant mass above 0.8 TeV and 1.3 TeV for an hypothesized Z' boson mass of 1.0 and 1.5 TeV respectively. Calling these expected numbers s and b, respectively, the significance S is obtained via the following estimator:

$$S = \sqrt{2((s+b)\ln(1+s/b)-s)} \tag{4}$$

which gives a good approximation to the likelihood-ratio based significance in the low statistics regime. To estimate the luminosity needed to have a 5 sigma evidence the Profile Likelihood Calculator [12–14] from RootStat tools was used. The uncertainty of the background is introduced directly in the method, while the uncertainty of the signal is incorporated by the use of MC convolution. Low limits in the dilepton invariant mass of 0.8 TeV and 1.3 TeV were used to estimate the significance for the Z' boson of 1.0 TeV and 1.5 TeV respectively. Table 2 shows the expected signal and background cross sections, in fb, at center-of-mass energy of 7 TeV after event selection in the Z' analysis.

Process	$M_{Z'} = 1.0$ TeV	$M_{Z'} = 1.5$ TeV
$Z' \to ee$	58.0(8)	5.73(11)
$Z \to ee$	1.86(2)	0.129(2)
$t\bar{t} \to ee$	0.08(6)	~ 0
$Z' \to \mu\mu$	59.6(8)	5.87(11)
$Z \to \mu\mu$	2.04(2)	0.139(2)
$t\bar{t} \to \mu\mu$	0.12(7)	~ 0

Table 2: Expected signal and background cross sections, in fb, at $\sqrt{s}$= 7 TeV, after event selection in the Z' analysis. Numbers in parenthesis show the uncertainties in the last digit.

Figure 10 shows the amount of integrated luminosity that would be required to observe a signal with a statistical significance of 5σ, as a function of the mass of the Z' boson. Even for integrated luminosities of $O(100\ \text{pb}^{-1})$, a Z' boson with a mass slightly above the current limit (1 TeV) could be found with a statistical significance above 5σ; with 1 fb^{-1}, masses of around 1.5 TeV can be reached. The plot shows also the integrated luminosity needed to obtain 10 signal events.

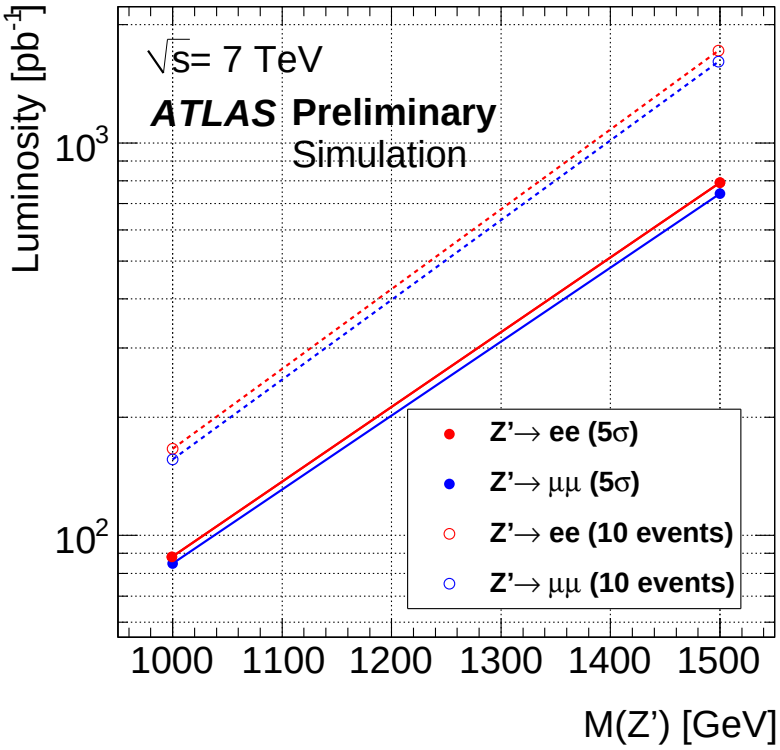

Figure 10: Integrated luminosity expected to yield ten signal events or a 5σ excess for a Z' signal.

6.3 Limits

If no resonance is found in the invariant mass distribution in the data, exclusion limits can be imposed on the production rate of the SSM Z' boson as a function of its mass. The expected 95% CL limits of this analysis were obtained using the algorithm described in [15], which allows the inclusion of uncorrelated systematic uncertainties on the expected signal and background rates. To evaluate the effect of correlated systematic uncertainties, a toy Monte Carlo study was done, in which the above algorithm was used repeatedly with signal and background values that varied together. Figure 11 shows the amount of integrated luminosity that is needed to set a 95% CL exclusion limit, as a function of the (SSM) Z' mass.

From the plot, it can be easily seen that the effect of systematic uncertainties is relatively small. The amount of expected background at the luminosity which is sufficient to set the limit is very small ($\sim$0.05 events in each channel). Therefore, in the majority of the performed experiments, the recorded background events will be 0. The probability to observe 1 background event instead of 0 (approximately 10% of the cases) will affect the limit as shown by the shaded area in Fig. 11. This fluctuation corresponds to roughly 2 Gaussian sigmas and is labeled accordingly in the plot; the plot does not show a 1σ band because a statistical fluctuation of the background cannot be less than one event.

Figure 12 shows the rate (cross section times branching ratio) of this channel that is expected to be excluded for different luminosities. These limits refer to the cross section expected around the resonance.

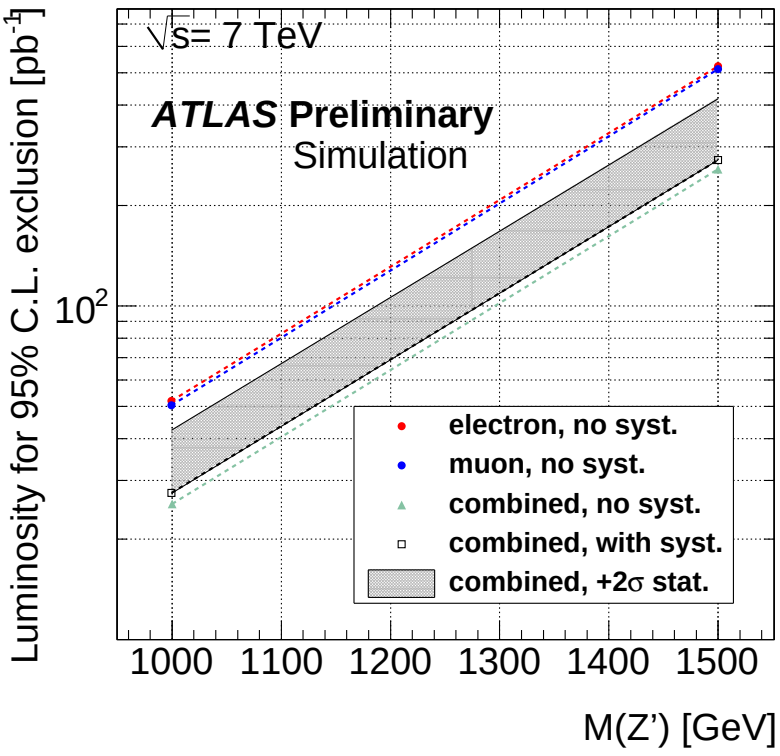

Figure 11: Integrated luminosity expected to allow a 95% CL exclusion of the SSM Z' model, as a function of $M(Z')$.

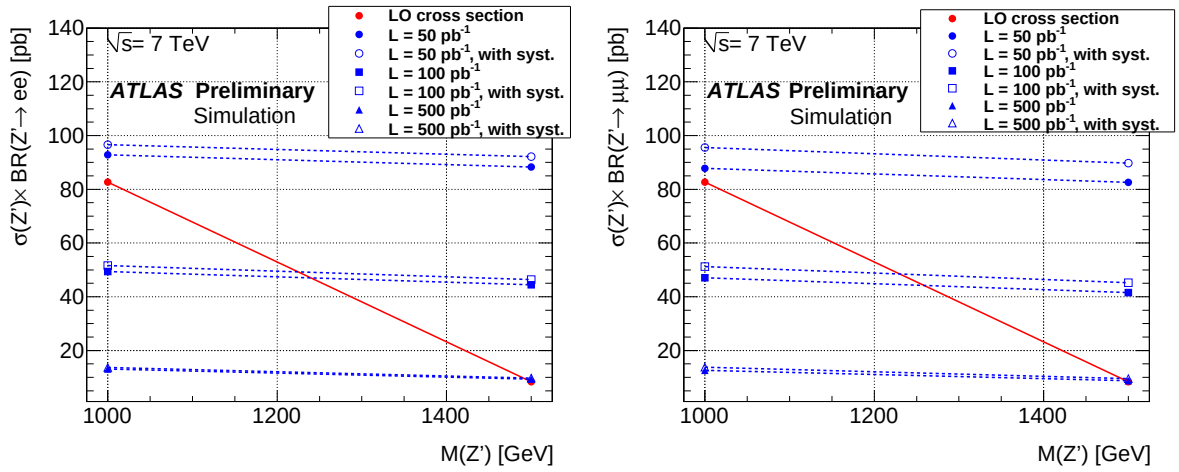

Figure 12: 95% C.L. exclusion limits on the Z' production cross section for the dielectron (left) and dimuon (right) channels.

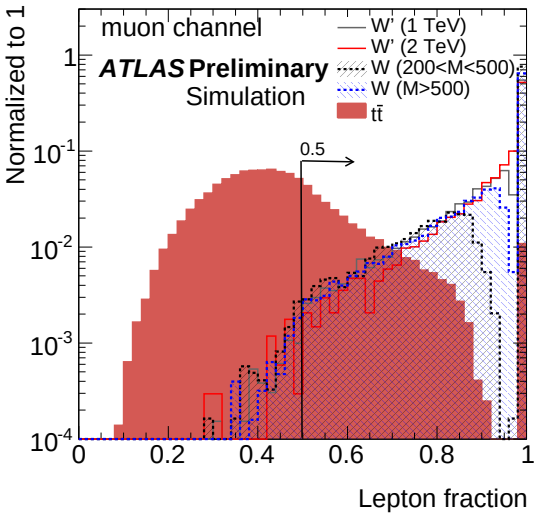

Figure 13: Distribution of the lepton fraction for W' bosons, SM W background and $t\bar{t}$ background.

7 Lepton+$\not{E}_T$ search potential

7.1 Event selection

The decay $W' \to \ell\nu$ provides a rather clean signature consisting of a single high-energy lepton and large missing transverse energy due to the undetected neutrino. A simple selection based on these quantities, plus quality criteria on the leptons (as described in Sections 3.1 and 3.2) can effectively reject the backgrounds of this search.

After applying electron and muon identification criteria, events are required to have:

- Only one reconstructed lepton with $p_T > 50$ GeV, within $|\eta| < 2.5$.
- Missing transverse energy $\not{E}_T > 50$ GeV.
- For the selected lepton, $\sum_{\Delta R<0.3} p_T^{tracks}/p_T^{lepton} < 0.05$

After these preselection cuts, the $t\bar{t}$ and dijet backgrounds can be further reduced, with a small effect on the signal rate, through the use of a *jet veto* cut and a cut on the *lepton fraction*. The *jet veto*, used for the electron channel, consists in rejecting events that contain any jet with a p_T above 200 GeV in a pseudorapidity region of $|\eta| < 2.5$. The *lepton fraction*, f_l, is defined as

$$f_l \equiv \frac{p_T^l + \not{E}_T}{p_T^l + \not{E}_T + \sum p_T^{\text{jets}}}$$

where p_T^l is the transverse momentum of the single lepton in the event. The jets entering the calculation must have $p_T > 40$ GeV and $|\eta| < 2.5$. The distribution of this variable is shown in Fig. 13 for several signal and background samples. As illustrated, the cut $f_l > 0.5$ rejects a large fraction of the $t\bar{t}$ background, while only barely affecting the W' boson signal.

The transverse momentum, p_T, of the single lepton in the event and the missing transverse energy $\not{E}_T$ are combined to obtain the *transverse mass* as follows:

$$m_T = \sqrt{2 p_T \not{E}_T (1 - \cos\Delta\phi_{l\not{E}_T})} \tag{5}$$

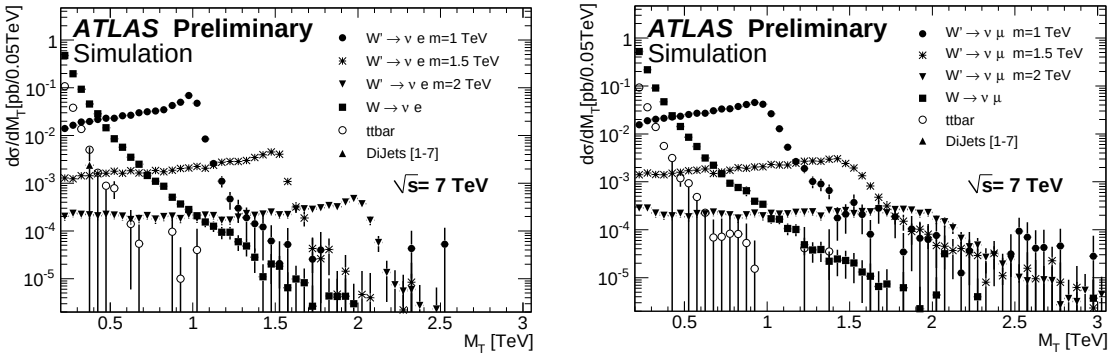

Figure 14: Transverse mass spectra after all cuts. Left, right: electron, muon channel.

where $\Delta\phi_{l\not{E}_T}$ is the angle between the lepton and the missing momentum in the transverse plane. Figure 14 shows the transverse mass distributions after cuts, with the reducible backgrounds well below the SM W tail at high transverse mass values. Clearly, a transverse mass cut provides a strong discrimination between the signal and the remaining backgrounds. The value of this cut was optimized with respect to the discovery significance. In a sliding window strategy, where several values of the true W' boson mass are tested, the largest significance is obtained when the cut is chosen at 70% of the hypothesized $m_{W'}$.

For the electron channel, either a single electron (with 10 GeV threshold) or a $\not{E}_T$ trigger (with a 30 GeV $\not{E}_T$ threshold) can be used very effectively to select the signal with 99% efficiency for the events that pass the analysis criteria. The single muon trigger has a lower efficiency for the muon channel due to the geometrical acceptance of the muon trigger chambers, leading to an efficiency of 86% for the selected events with a 10 GeV threshold. Table 3 shows the expected signal and background cross sections, in fb, at center-of-mass energy of 7 TeV after event selection in the W' analysis.

Process	$M_{W'} = 1.0\ TeV$	$M_{W'} = 1.5\ TeV$	$M_{W'} = 2.0\ TeV$
$W' \to e\nu$	320(5)	34.5(5)	4.32(6)
$W \to e\nu$	5.68(8)	0.66(6)	0.077(15)
$t\bar{t} \to e\nu$	0.2(1)	$\sim$0	~ 0
$W' \to \mu\nu$	287(4)	28.6(4)	3.83(5)
$W \to \mu\nu$	5.03(8)	0.60(6)	0.085(17)
$t\bar{t} \to \mu\nu$	0.9(3)	0.03(2)	~ 0

Table 3: Expected signal and background cross sections, in fb, at $\sqrt{s}$= 7 TeV, after all steps of event selection in the W' analysis. Numbers in parenthesis show the uncertainties in the last digit(s).

7.2 Luminosity for discovery

Using the significance estimator presented in Section 6.2, the expected luminosity needed for a 5σ signal significance is presented in Fig. 15 for the two channels and for a combined search. The figure also presents the luminosity needed to find 10 signal events for a W' boson with a production cross section given by the benchmark model used.

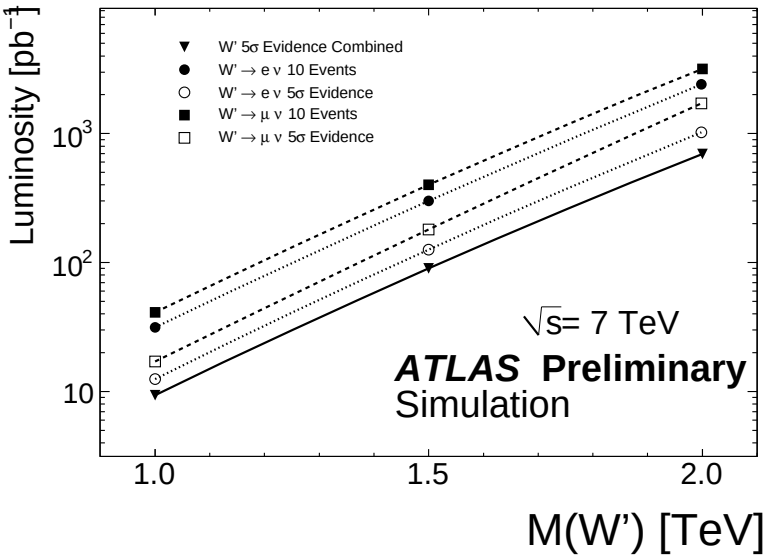

Figure 15: Integrated luminosity expected to yield ten signal events or a 5σ significance for a W' signal (benchmark model).

7.3 Limits

In case no W' boson is discovered in the 7 TeV data, exclusion limits can be imposed following the same procedure described in Section 6.3. Figure 16 shows the amount of integrated luminosity needed to set a 95% CL exclusion limit on the benchmark W' model, as a function of the W' mass. Also in this case, a one-event fluctuation of the background is already above the 1σ level. The shaded area corresponds to a 2σ statistical uncertainty of the median expected luminosity to set the limit. Figure 17 shows, equivalently, the rate (cross section times branching ratio) of this channel that is expected to be excluded for different luminosities.

8 Summary and conclusions

The ATLAS potential for the discovery or exclusion of Z' and W' bosons through their leptonic decays has been estimated for a center-of-mass energy of 7 TeV. A W' resonance could be observed with a statistical significance of 5σ with an integrated luminosity of about 20 pb^{-1} if its mass is not far above 1 TeV, which is the current 95% CL exclusion limit set by Tevatron. With an integrated luminosity as low as 10 pb^{-1}, it may be possible to match this limit. A luminosity of 50 pb^{-1} would allow ATLAS to exclude this benchmark model up to a mass of 1.5 TeV, while 1 fb^{-1} would extend the exclusion up to 2 TeV.

A Z' dilepton resonance could be observed with a statistical significance of 5σ with an integrated luminosity of about 100 pb^{-1} if its mass is not far above 1 TeV. This integrated luminosity would also be enough to extend the exclusion to about 1.3 TeV. An integrated luminosity of around 50 pb^{-1} may be enough to match the current 95% CL exclusion limit of 1 TeV, set by Tevatron for the SSM Z' boson.

References

[1] G. Altarelli, B. Mele, M.Ruiz-Altaba, Z. Phys. **C45** (1989) 109.

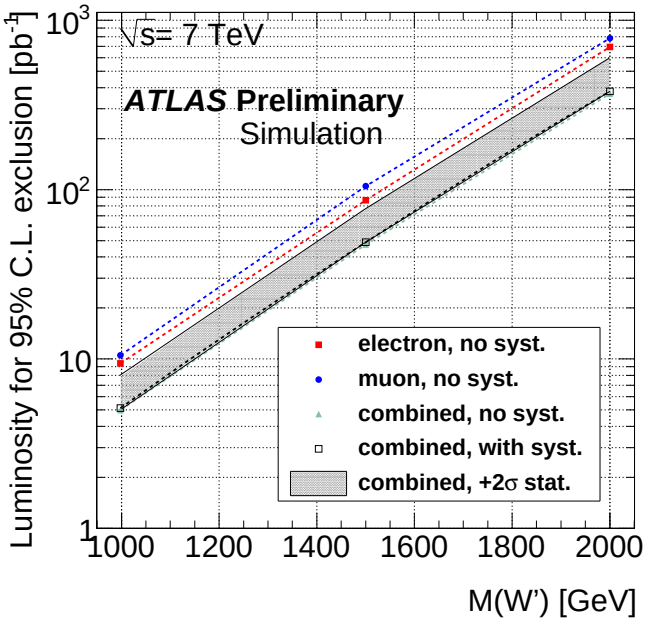

Figure 16: 95% C.L. exclusion limits on the W' production cross section, assuming the same branching ratio for all leptons.

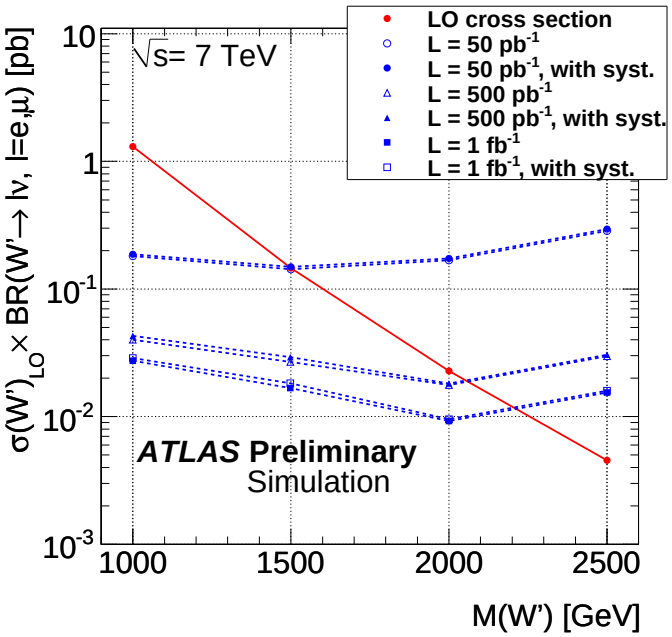

Figure 17: 95% C.L. exclusion limits on the W' production cross section, assuming the same branching ratio for all leptons.

[2] V.M. Abazov et al. (DØ Collaboration), Phys. Rev. Lett. **100** (2008) 31804.

[3] T. Aaltonen et al. (CDF Collaboration), Phys. Rev. Lett. **102** (2009) 091805.

[4] ATLAS Collaboration, Detector and Physics Performance Technical Design Report, CERN-LHCC/99-14, 1999.

[5] ATLAS Collaboration, Expected performance of the ATLAS experiment : detector, trigger and physics, CERN-OPEN-2008-020; arXiv:0901.0512, 2009.

[6] T. Sjostrand, S. Mrenna, and P. Skands, JHEP 0605:026,2006, hep-ph/0603175.

[7] S. Frixione and B.R. Webber, JHEP 0206:029,2002, hep-ph/0204244.

[8] J. Pumplin, D.R. Stump, J. Huston, H.L. Lai, P. Nadolsky, W.K. Tung, : JHEP 0207:012,2002, hep-ph/0201195.

[9] ATLAS Collaboration, Commissioning of the ATLAS Muon Spectrometer with Cosmic Rays, ATLAS-MUON-2010-01-003, to be submitted to EPJC, 2010.

[10] J. M. Campbell and R. K. Ellis, Phys. Rev. D **62** (2000) 114012.

[11] M.R. Whalley, D. Bourilkov, R.C. Group, http://hepforge.cedar.ac.uk/lhapdf/.

[12] K. Cranmer, arXiv:physics/0511028v2.

[13] R. D. Cousins, J. T. Linnemann, J. Tucker, arXiv:physics/0702156v4.

[14] K.S. Cranmer, CERN-2008-001, Statistical Issues for LHC Physics p47-60.

[15] T. Junk, Confidence Level Computation for Combining Searches with Small Statistics, 1999, Nucl.Instrum.Meth.A434:435-443.